ELSEVIER

Inorganica Chimica Acta 226 (1994) 259–265

Inorganica Chimica Acta

Redox reactions between oxomolybdenum(IV) and tetratolylporphinatoiron(III) complexes

Michael J. LaBarre, Andrew Pacheco, John H. Enemark *

Department of Chemistry, University of Arizona, Tucson, AZ 85721, USA

Received 3 May 1994

Abstract

The coupling of an $Mo^{VI}O_2 \rightarrow Mo^{IV}O$ oxygen atom transfer reaction to a one-electron reoxidation of the resulting Mo(IV) center by an Fe(III) porphyrin center has been investigated in an attempt to model the first two redox steps in the catalytic cycle of the enzyme sulfite oxidase. Reaction of $LMo^{VI}O_2Cl$ (L = hydrotris(3,5-dimethyl-1-pyrazolyl)borate) with excess triphenylphosphine in DMF rapidly and cleanly generates $LMo^{IV}OCl(DMF)$. This Mo(IV) species reacts more slowly with $Fe^{III}Cl(TTP)$ (TTP = tetratolylporphyrin) to give $LMo^{V}OCl_2$ and $Fe^{II}(TTP)$ as the final products. The kinetics of this one-electron redox reaction have been followed by electronic spectroscopy and by ^1H NMR. The reaction is zero-order in Fe(III), first-order in Mo(IV), and independent of added chloride ion. The first-order rate constant determined by these methods ranged from $1.7–4.6 \times 10^{-5}$ s^{-1}. An inner-sphere (halogen transfer) mechanism is shown to be most consistent with the data.

Keywords: Tetratolylporphinatoiron(III) complexes; Oxomolybdenum complexes; Redox reactions; Kinetics

1. Introduction

The proposed catalytic cycle for sulfite oxidase, an essential pterin-containing molybdenum enzyme [1] that catalyzes the oxidation of sulfite to sulfate, is shown in Fig. 1 [2]. The fully oxidized enzyme is thought to transfer an oxygen atom from a dioxo–Mo(VI) center to sulfite to produce sulfate and a reduced monooxo–Mo(IV) center. Regeneration of the dioxo–Mo(VI) center involves two successive one-electron intramolecular electron transfer reactions (A and B) from the Mo(IV or V) center to the Fe(III) state of the b-type heme. After each intramolecular transfer step the b-type heme center is reoxidized by the biological electron transfer protein cytochrome *c*. Oxygen atom transfer reactions are well known for model molybdenum complexes [3], and the model system $LMoO_2(SPh)$ has been shown to catalyze the oxidation of PPh_3 by oxygen in the presence of trace amounts of water via a sequence of atom transfer and coupled electron–proton transfer reactions that are similar to those proposed for the molybdenum centers of enzymes [4]. The goal of this study was to chemically mimic the first two steps of the sulfite oxidase reaction cycle of Fig. 1 by coupling an $Mo^{VI}O_2 \rightarrow Mo^{IV}O$ oxygen atom transfer reaction to a one-electron reoxidation of the resulting Mo(IV) center by an Fe(III) porphyrin (step A).

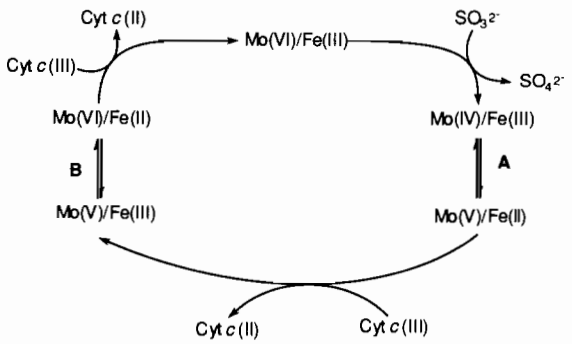

Fig. 1. Proposed catalytic cycle for sulfite oxidase, adapted from Ref. [2]. **A** is the intramolecular electron transfer reaction for the two-electron reduced state of the enzyme. **B** is the intramolecular electron transfer reaction for the one-electron reduced state.

2. Experimental

2.1. Materials

Reactions were carried out under an atmosphere of dry argon unless specified otherwise. Subsequent work-

* Corresponding author.

SSDI 0020-1693(94)04094-C

ups of anaerobic reactions were carried out in air. All reagents were used as received unless otherwise noted. Solvents were treated in the following manners: dimethylformamide (DMF) was stored over 4 Å molecular sieves; dichloromethane and dichloroethane were distilled from calcium hydride; ethanol was distilled from calcium oxide; toluene was distilled from sodium. Triphenylphosphine (PPh_3) and tetrabutylammonium tetrafluoroborate were recrystallized from ethanol. Chromatography was conducted using glass columns wet-packed with either silica gel (Sigma, S-2509) or neutral activated alumina. Potassium hydrotris(3,5-dimethyl-1-pyrazolyl)borate (KL) [5] and [hydrotris(3,5-dimethyl-1-pyrazolyl)borato]dichlorooxomolybdenum(V) ($LMo^{V}OCl_2$) [6] were prepared according to literature methods. [Hydrotris(3,5-dimethyl-1-pyrazolyl)borato]chlorodioxomolybdenum(VI) ($LMo^{VI}O_2Cl$) [7], [hydrotris(3,5-dimethyl-1-pyrazolyl)borato]chloro(dimethylformamido)oxomolybdenum(IV) ($LMo^{IV}OCl(DMF)$) [7], 5,10,15,20-tetra-*p*-tolylporphyrin (TTP) [8], and chloro-5,10,15,20-tetra-*p*-tolylporphinatoiron(III) ($Fe^{III}Cl(TTP)$) [9,10] were prepared by modifications of the published procedures.

2.2. Physical measurements

Cyclic voltammetry was performed using an IBM EC/225 potentiostat and a normal three-electrode configuration. The reference electrode was a saturated calomel electrode (SCE) with a platinum disk working electrode and a platinum wire counter electrode. The sample concentration was approximately 1 mM and the supporting electrolyte was tetrabutylammonium tetrafluoroborate at 100 mM. All half-wave potentials were referenced against the ferrocenium/ferrocene couple. ^1H NMR spectra were recorded on a Bruker AM-500 spectrometer. Electronic spectra were recorded on a modified Cary 14 spectrophotometer equipped with an OLIS interface and software. Electron paramagnetic resonance (EPR) measurements were obtained with a Varian E-3 spectrometer. Room temperature EPR spectra were referenced to external diphenylpicrylhydrazide (DPPH). Low temperature spectra were obtained with a liquid nitrogen sample Dewar. Samples in DMF were measured at room temperature with a thin-layer cell and at low temperature by diluting with an equal volume of dry toluene and utilizing normal 5 mm quartz tubes. All manipulations requiring anaerobic conditions were completed utilizing normal Schlenk and cannula techniques.

2.3. Kinetic measurements

Kinetics were measured in DMF, and the reactions were followed by both visible and NMR spectroscopies. Solutions were equilibrated to 25 °C prior to use and were maintained to within ±0.5 °C with a circulating propylene glycol bath and modified cuvette holders. The ^1H NMR measurements were made on a Bruker AM-500 spectrometer equipped with a Bruker temperature controller. The actual probe temperature was checked by calibration with both ethylene glycol and methanol and is accurate to ±0.5 °C.

Care was taken to be as consistent as possible in all runs. Solutions of $LMo^{VI}O_2Cl$ and $Fe^{III}Cl(TTP)$ were premixed in septa sealed cuvettes or NMR tubes. These solutions were then degassed for at least 15 min by a stream of bubbling argon. Triphenylphosphine solutions were prepared and degassed separately. PPh_3 was added with a microsyringe such that the total volume change was always less than 5% and the $[PPh_3]/[LMo^{VI}O_2Cl]$ ratio was at least 5. This method generated the reduced Mo(IV) species, $LMo^{IV}OCl(DMF)$, within the mixing time (< 1 min). Actual experimental concentrations and subsequent data workup were dependent upon the solvent used and the spectroscopic method utilized to follow the reaction.

3. Results

3.1. Oxygen atom transfer reaction in DMF

Oxygen atom transfer reactions of the type $[Mo^{VI}O_2]^{2+}$ to $[Mo^{IV}O]^{2+}$ are well known [3] and the specific oxo-transfer chemistry of $LMo^{VI}O_2Cl$ has been well studied [7]. Reaction of $LMo^{VI}O_2Cl$ with excess PPh_3 in coordinating solvents (Sol) yields $LMo^{IV}OCl(Sol)$ as the only molybdenum-containing product. ^{31}P NMR spectroscopy confirms that 1 mol of $OPPh_3$ is produced per mol of $LMo^{VI}O_2Cl$ reacted with PPh_3. The crystal structure of $LMo^{IV}OCl(pyridine)$ [7] has been determined and shows that the ligands are arranged in a distorted octahedral geometry with facial coordination of the polypyrazolylborate ligand. The pyridine molecule is *cis* to both the chloro and oxo ligands.

The reaction of $LMo^{VI}O_2Cl$ with excess PPh_3 in DMF is complete in < 1 min when PPh_3 is present in a five-fold excess. The green product, $LMo^{IV}OCl(DMF)$, has a broad visible absorbance maximum at 790 nm ($\epsilon \sim 120\ M^{-1}\ cm^{-1}$), characteristic of a $[Mo^{IV}O]^{2+}$ d–d transition [11]. The visible spectrum remained constant for at least 5 days under an anaerobic environment. The product, $LMo^{IV}OCl(DMF)$, is apparently not reactive towards water (see below).

The reaction of $LMo^{VI}O_2Cl$ with PPh_3 to generate $LMo^{IV}OCl(Sol)$ is easily monitored by ^1H NMR spectroscopy in DMF-d_7. The C_s symmetry of the parent $LMo^{VI}O_2Cl$ results in proton singlets of intensities 1:2:6:3:6:3 that are assignable to the three pyrazolylborate ring protons and the eighteen protons of the methyl groups. The product, $LMo^{IV}OCl(DMF)$, has no

symmetry and gives proton resonances that are in the ratio of 1:1:1:3:6(br):3:3:3. This spectrum of $LMo^{IV}OCl(Sol)$ is stable under anaerobic conditions and is independent of the amount of water present (integrations of the proton signals suggest an H_2O:$LMo^{IV}OCl(DMF)$ ratio of at least 10:1 in the NMR experimcnts). The final proton NMR spectrum is similar to that obtained for $LMo^{IV}OCl(pyridine)$ [11].

Reversible one-electron reductions of $[Mo^{VI}O_2]^{2+}$ centers to $[Mo^{V}O_2]^{1+}$ are rare and only occur when there is sufficient steric bulk around the metal center to prevent dimer formation [12–14]. One-electron reduction of $[Mo^{VI}O_2]^{2+}$ usually results in the loss of one of the terminal oxo ligands and subsequent dimer formation. $LMo^{VI}O_2Cl$ displays completely irreversible electrochemical behavior when studied by cyclic voltammetry in DMF. The cyclic voltammogram of the reduced product from the oxo-transfer reaction, $LMo^{IV}OCl(DMF)$, however, displays pseudo-Nernstian behavior in DMF at +93 mV versus SCE (Table 1), that can be assigned to the $[LMo^{V}OCl(DMF)]^{1+}$/$LMo^{IV}OCl(DMF)$ redox couple. Comparison of the peak currents of equimolar solutions of $LMo^{IV}OCl(DMF)$ and $LMo^{V}OCl_2$ [6] confirms that the oxidation of $LMo^{IV}OCl(DMF)$ is a one-electron process.

3.2. Electron/halogen transfer reaction in DMF

The reactions of $LMo^{VI}O_2Cl$ and $Fe^{III}Cl(TTP)$ with PPh_3 were studied under anaerobic conditions in DMF. $LMo^{IV}OCl(DMF)$ was generated in situ by the addition of excess PPh_3 (at least five-fold) to a solution containing both $LMo^{VI}O_2Cl$ and $Fe^{III}Cl(TTP)$. Under the conditions used in these experiments $Fe^{III}Cl(TTP)$ is unreactive toward PPh_3 or $OPPh_3$, and no differences were detected in either the ^1H NMR or UV–Vis spectrum of $Fe^{III}Cl(TTP)$ in the presence of a 100-fold excess of PPh_3 or $OPPh_3$.

The reaction of $LMo^{VI}O_2Cl$ with excess PPh_3 is complete within 1 min. This fast reaction is followed by a much slower reaction between $LMo^{IV}OCl(DMF)$ and $Fe^{III}Cl(TTP)$. The slow reaction was monitored under anaerobic conditions in DMF by UV–Vis, EPR and NMR spectroscopies. In the presence of a 4:1 ratio of $LMo^{IV}OCl(DMF)$:$Fe^{III}Cl(TTP)$ [1] the spectrum of $Fe^{III}Cl(TTP)$ with λ_{max} at 508 and 570 nm is slowly converted to a spectrum with λ_{max} at 535(sh), 568 and 608 nm (Fig. 2). This conversion requires less than 5 h under these reaction conditions. An isosbestic point at 530 nm is observed throughout the course of the reaction, indicating that only two absorbing species are present. The final spectrum is identical to that previously published for $Fe^{II}(TTP)$ in DMF [15–18]. EPR measurements of the final reaction mixture indicated the presence of only one EPR-active species in the room temperature spectrum with $\langle g \rangle = 1.947$ and $^{95,97}Mo\langle A \rangle = 46 \times 10^{-4}$ cm^{-1}. These EPR parameters are identical to those for $LMo^{V}OCl_2$ [6], and the EPR spectrum after completion of the reaction was superimposable with the spectrum of an authentic sample of $LMo^{V}OCl_2$. No other reaction products were detected by EPR, UV–Vis or NMR spectroscopy.

3.3. Kinetics of the reaction in DMF

The kinetics of the reaction at 25 °C between $LMo^{IV}OCl(DMF)$ and $Fe^{III}Cl(TTP)$ in DMF were investigated under pseudo-first-order conditions. A 10- to 25-fold excess of $LMo^{IV}OCl(DMF)$ was quantitatively generated in solution from the reaction of excess PPh_3

Table 1
Half-wave reduction potentials of several Mo- and Fe-containing compounds in DMF

Redox couple	Half-wave potential [a] (V)
$[Fe^{III}(TTP)]^+/Fe^{II}(TTP)$ [b]	−0.02
$Fe^{III}Cl(TTP)/[Fe^{II}Cl(TTP)]^-$	−0.16
$[LMo^{V}OCl(DMF)]^+/LMo^{IV}OCl(DMF)$	+0.09
$LMo^{V}OCl_2/[LMo^{IV}OCl_2]^-$	−0.28

[a] Determined by cyclic voltammetry in DMF solutions and referenced to SCE. Compound concentration is approximately 1 mM. Supporting electrolyte is tetrabutylammonium tetrafluoroborate at 100 mM. Scan rate is 100 mV s^{-1}. All compounds exhibit pseudo-Nernstian behavior with i_{pc}/i_{pa} ratios ≈ 1.0.

[b] Value listed is actually the half-wave reduction potential for $Fe^{III}(ClO_4)(TTP)$ in DMF. In DMF this perchlorate iron(III) porphyrin is believed to exist entirely as a dissociated ion pair, $[(DMF)_2Fe^{III}(TTP)]^+ + ClO_4^-$.

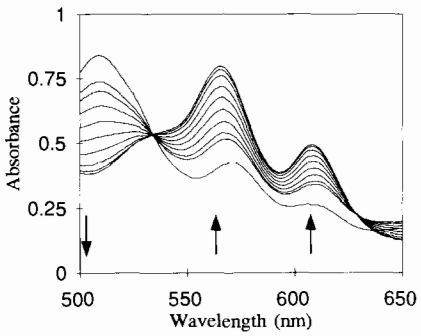

Fig. 2. Reduction of $Fe^{III}Cl(TTP)$ by $LMo^{IV}OCl(DMF)$ in DMF as monitored by visible spectral changes: $[LMo^{IV}OCl(DMF)]_{init} = 7.0 \times 10^{-4}$ M, $[Fe^{III}Cl(TTP)]_{int} = 6.2 \times 10^{-5}$ M. Each successive scan represents approximately 4 min of the reaction. Isosbestic point is at 535 nm.

[1] The initial absorbance spectrum of $Fe^{III}Cl(TTP)$ is unaffected by the presence of $LMo^{IV}OCl(DMF)$ over the range 475–600 nm due to the large differences in the extinction coefficients and a lack of Mo^{IV} absorbances in this region.

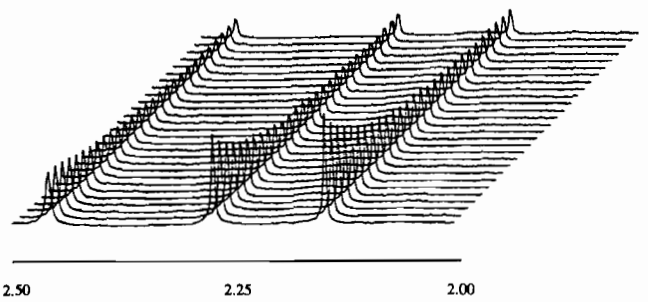

Fig. 3. ^{1}H NMR spectra of the reduction of $Fe^{III}Cl(TTP)$ by $LMo^{IV}OCl(DMF)$; $[LMo^{IV}OCl(DMF)] = 1.8$ mM, $[Fe^{III}Cl(TTP)] = 1.0$ mM. The resonances displayed correspond to three of the pyrazolyl methyl groups of $LMo^{IV}OCl(DMF)$. Spectra were recorded approximately every 64 min. Horizontal scale is chemical shift in ppm.

with $LMoO_2Cl$ as described above. The loss of absorbance from $Fe^{III}Cl(TTP)$ at 508 nm was followed in the electronic spectrum, and the process is zero-order with respect to Fe; the initial concentrations of $Fe^{III}Cl(TTP)$ ranged from 1×10^{-5} M to 1×10^{-4} M. Plots of k_{obs} (in M s^{-1}) versus $[LMo^{IV}OCl(DMF)]$ give an apparent first-order rate constant of 4.6×10^{-5} s^{-1} at 25 °C [19].

The reaction was also monitored by ^{1}H NMR spectroscopy. These experiments were not run under pseudo-first-order conditions due to detection and solubility limits. The initial concentration of $Fe^{III}Cl(TTP)$ was ≈ 1.0 mM and reactions were run at Fe:Mo ratios of 1:0.5, 1:1 and 1:2, at 25 °C. The signals assignable to $LMo^{IV}OCl(DMF)$ are fully formed within 5 min, the minimum time required to reinsert the sample, establish deuterium lock and collect a spectrum. The resonances of $LMo^{IV}OCl(DMF)$ disappear very slowly over time (Fig. 3), whereas the resonances due to $Fe^{III}Cl(TTP)$ and $Fe^{II}(TTP)$ are not able to be confidently followed due to probable spin exchange, solvent exchange, or electron–nuclear dipolar relaxation. Plots of $\ln([Mo^{IV}]_0/[Mo^{IV}]_t)$ versus time are linear to 85% of the reaction, indicating first-order behavior with respect to Mo, and yielding a rate constant of $1.7(5)\times10^{-5}$ s^{-1}. The rate constant computed from the NMR results is independent of the initial concentrations of either $LMo^{IV}OCl(DMF)$ or $Fe^{III}Cl(TTP)$. These observations are consistent with a reaction sequence which is zero-order with respect to Fe, as observed in the visible spectroscopy experiments.

4. Discussion

The overall reaction of $LMo^{VI}O_2Cl$ and $Fe^{III}Cl(TTP)$ with PPh_3 in DMF has been studied at 25 °C by UV–Vis, EPR and NMR spectroscopies. The initial fast oxo-transfer process is followed by a much slower electron/halogen exchange reaction between the now reduced $LMo^{IV}OCl(DMF)$ and $Fe^{III}Cl(TTP)$. The net reaction process is seen in reaction (1). UV–Vis spectra taken over the course of the reaction display an isosbestic point at 530 nm indicating the presence of only two absorbing species at this wavelength. These are clearly identified as $Fe^{III}Cl(TTP)$ and $Fe^{II}(TTP)$ in DMF based on comparison to the previously published spectra for both species [15–18].

$$LMo^{VI}O_2Cl + Fe^{III}Cl(TTP) + PPh_3 \xrightarrow{DMF} LMo^{V}OCl_2 + Fe^{II}(TTP) + OPPh_3 \quad (1)$$

The ^{1}H NMR studies of the initial oxygen atom transfer reaction of $LMo^{VI}O_2Cl$ with PPh_3 indicate the presence of only one reduced Mo(IV) product. This species is formulated as $LMo^{IV}OCl(DMF)$ by analogy to the previously isolated compound, $LMo^{IV}OCl$(pyridine). The oxo-transfer process is followed by reduction of the Fe(III) center with concomitant appearance of a room temperature EPR active species identified as $LMo^{V}OCl_2$. No other molybdenum or iron compounds have been detected during the reaction.

The overall process for reaction (1) is best described as a combination of two discrete steps. An initial fast oxygen atom transfer (reaction (2)) is followed by a subsequent slower electron/halogen exchange reaction.

$$LMo^{VI}O_2Cl + PPh_3 \xrightarrow{DMF} LMo^{IV}OCl(DMF) + OPPh_3 \quad (2)$$

The product of reaction (2), $LMo^{IV}OCl(DMF)$, is quantitatively formed within 2 min when a 10-fold excess of PPh_3 is added to a 1mM solution of $LMo^{VI}O_2Cl$ in DMF at 25 °C. This corresponds to an apparent limiting second-order rate constant of ≈ 6 M^{-1} s^{-1} (the assumption of a second-order process is based on the known reactions of similar $LMo^{VI}O_2X$ compounds where X = OPh, SPh, etc.) [7]. This rate, when correlated to a first-order process at the concentrations employed in these experiments, is 2–3 orders of magnitude faster than the subsequent electron/halogen exchange process depicted in reaction (3) and discussed below.

$$LMo^{IV}OCl(DMF) + Fe^{III}Cl(TTP) \xrightarrow{DMF} LMo^{V}OCl_2 + Fe^{II}(TTP) \quad (3)$$

The fast initial oxygen atom transfer reaction allowed the kinetics of reaction (3) to be determined in situ by the addition of PPh_3 to a solution of $LMo^{VI}O_2Cl$ and $Fe^{III}Cl(TTP)$. This reaction was studied by several methods and found to be zero-order in Fe and first-order in Mo.

4.1. Mechanism of the electron/halogen transfer reaction in DMF

The zero-order dependence on Fe of the electron/halogen transfer reaction is a key observation to be

kept in mind when proposing a mechanism. From this observation, it follows that only the molybdenum center is involved in the rate-determining step; i.e. the electron-transfer step cannot be rate-determining. This fact immediately eliminates a simple outer-sphere mechanism involving direct electron transfer from Mo^{IV}-OCl(DMF) to the Fe^{III} center. A plausible mechanism consistent with the kinetic data is shown in Scheme 1.

According to this mechanism, electron transfer from the molybdenum to the iron occurs rapidly via a chlorine atom bridge, to give the observed products, $LMo^{V}OCl_2$ and $Fe^{II}(TTP)$. This process can be described as an inner-sphere electron transfer reaction from Mo(IV) to Fe(III) or as a chlorine atom transfer reaction. Chlorine atom transfer reactions involving oxo compounds of tungsten, molybdenum and rhenium are well documented [20,21]. $LMo^{IV}OCl(DMF)$ is coordinatively saturated and unreactive towards chlorine atom transfer, so the redox step must be preceded by a slow dissociation of DMF from the Mo complex.

The role of axially bound ligands in both inner- and outer-sphere electron transfer processes has been a continuing area of interest in both synthetic as well as naturally occurring porphyrin systems [22,23]. Oxide groups have long been known to act as bridging groups between iron centers in porphyrins, facilitating both magnetic and electronic interactions [24,25]. Chloro [26–28], azido [29], nitrido [28,30], and cyano [31,32] ligands have also been shown to participate in both inner- and outer-sphere transfer reactions.

The reaction between $Fe^{III}Cl(TTP)$ and $Cr^{II}(acac)_2$ (where acac is 2,4-pentanedione) was studied anaerobically in benzene–pyridine (1%) using radiolabeling techniques [26,27]. $Fe^{III}Cl(TTP)$ was shown to be inert with respect to ionic chloride transfer indicating that in this solvent system $Fe^{III}Cl(TTP)$ exists as the axially bound chloride monomer. Transfer experiments using $Fe^{III}Cl^{*}(TTP)$ as the chlorine transfer source to $Cr^{II}(acac)_2$ performed in the presence of ionic chloride indicated at least 87% transfer of the Cl^{*} to the Cr^{III} products. No attempt was made to fully identify the chromium products, but the final iron product was shown to be $[Fe^{III}(TTP)]_2O$, presumably formed during the aerobic workup of the reaction. Thus, the halogen transfer reaction proceeds via an inner-sphere process.

Electron self-exchange in cobalt porphyrins has also been shown to be facilitated by bridging chlorine atoms [31,32]. The inner-sphere electron exchange between $Co^{III}Cl(TTP)$ and $Co^{II}(TTP)$ was studied by ^1H NMR in various solvents. The results indicate that inner-sphere transfer is 4–6 orders of magnitude faster than the corresponding outer-sphere exchanges for the analogous pyridine complexes. The enhancement in rates is assignable to the smaller inner-sphere reorganization energy required to change the conformations of reactants to those of the activated complex and to an overall smaller solvent reorganizational energy. Recent work utilizing nitrido axial ligands [28,30] indicates the possibility of metalloporphyrins participating in net two- and three-electron redox processes.

The individual half-wave reduction potentials (Table 1) show that the driving force for an outer-sphere electron transfer reaction mechanism of $Mo^{IV}OCl(DMF)$ with $ClFe^{III}(TTP)$ or with $Fe^{III}(TTP)^+$ would be unfavorable. The driving force for reaction (3) is the formation of a Mo–Cl bond in the postulated inner-sphere mechanism (Scheme 1).

Although the inner-sphere mechanism described in Scheme 1 provides a good explanation for the experimental data, one cannot immediately rule out an outer-sphere mechanism such as the one shown in Scheme 2. From Table 1, it is clear that step 4 of Scheme 2 would be very favorable thermodynamically, and would provide the driving force for the reaction.

The nature of $Fe^{III}Cl(TTP)$ in DMF has been studied by electrochemical techniques [33–38]. Cyclic voltammetry indicates that at concentrations from 0.1 to 1.0 mM the only axial ligand present on $Fe^{III}Cl(TTP)$ in DMF is the chloride ion. However, there is clear evidence for chloride loss from the reduced iron species $[Fe^{II}Cl(TTP)]^-$. One cathodic process is observed during the negative potential sweep, but one or two peaks are observed during the reverse sweep, depending upon the sweep rate. Slow scans (25 mV s^{-1}) result in one

1. $LMo^{IV}OCl(DMF) \xrightarrow{slow} LMo^{IV}OCl + DMF$

2. $LMo^{IV}(=O)(Cl) + Fe^{III}Cl(TTP) \xrightarrow{fast} [LMo^{IV}(=O)(Cl)\text{---}Cl\text{–}Fe^{III}(TTP)]$

3. $[LMo^{IV}(=O)(Cl)\text{---}Cl\text{–}Fe^{III}(TTP)] \xrightarrow{fast} [LMo^{V}(=O)(Cl)\text{–}Cl\text{---}Fe^{II}(TTP)]$

4. $[LMo^{V}(=O)(Cl)\text{–}Cl\text{---}Fe^{II}(TTP)] \xrightarrow{fast} LMo^{V}OCl_2 + Fe^{II}(TTP)$

Scheme 1. The proposed inner-sphere mechanism for the electron/halogen transfer reaction between $Fe^{III}Cl(TTP)$ and $LMo^{IV}OCl(DMF)$; step 1 is rate-determining.

1. $Fe^{III}(TTP)Cl \overset{fast}{\rightleftharpoons} [Fe^{III}(TTP)]^+ + Cl^-$

2. $LMo^{IV}OCl(DMF) \underset{k-1}{\overset{k1}{\rightleftharpoons}} LMo^{IV}OCl + DMF$

3. $LMo^{IV}OCl + Cl^- \xrightarrow{k2} [LMo^{IV}OCl_2]^-$

4. $[LMo^{IV}OCl_2]^- + [Fe^{III}(TTP)]^+ \xrightarrow{fast} LMo^{V}OCl_2 + Fe^{II}(TTP)$

Scheme 2. An alternative outer-sphere electron transfer mechanism for reaction (2).

broadened anodic peak. At increased scan rates (>50 mV s^{-1}), this anodic wave splits into two peaks with the more positive one corresponding to that observed for $Fe^{III}(TTP)(ClO_4)$, which exists solely as a separated ion pair in DMF solutions [39]. Thus, the more negative anodic process is assigned to an $Fe^{III}Cl(TTP)/[Fe^{II}Cl(TTP)]^-$ redox couple whereas the more positive process is probably due to the $[Fe^{III}(TTP)]^+/Fe^{II}(TTP)$ couple arising from chloride loss from the above anion. Conductivity studies indicate that at ≈1 mM, solutions of $Fe^{III}Cl(TTP)$ in DMF behave as non-electrolytes. As the $Fe^{III}Cl(TTP)$ concentration is lowered the conductivity increases; plots of $[Fe^{III}Cl(TTP)]$ versus molar conductance are linear and indicate that at low concentrations $Fe^{III}Cl(TTP)$ behaves as a weak one to one electrolyte [33].

UV–Vis studies as a function of the concentration of $Fe^{III}Cl(TTP)$ in DMF have indicated the presence of different chromophores at varying Fe(III) concentrations. At low $[Fe^{III}Cl(TTP)]$ ($\sim 5\times10^{-5}$ M) the spectrum is identical to that observed for the compound in DMSO where $Fe^{III}Cl(TTP)$ exists as a completely dissociated ion pair [40]. As the concentration is raised to about 1×10^{-3} M the spectrum is transformed into one identical to that of $Fe^{III}Cl(TTP)$ in CH_2Cl_2, where $Fe^{III}Cl(TTP)$ is thought to exist completely as the coordinated halide complex [33,41].

Thus, at the $Fe^{III}(TTP)Cl$ concentrations employed in our work (10^{-4}–10^{-5} M), a significant amount of chloride dissociation, as shown in step 1 of Scheme 2, is anticipated. The complete rate law for the mechanism depicted in Scheme 2 is given by Eq. (4). In practice, this can be simplified further. DMF is the solvent for the reaction, and will be present at the concentration of 12.5 M. The concentration of Cl^-, by contrast,

$$\frac{d[Fe^{II}]}{dt} = \frac{k_1k_2[LMo^{IV}OCl(DMF)][Cl^-]}{k_{-1}[DMF]+k_2[Cl^-]} \quad (4)$$

can be at most 10^{-4} M, assuming that $Fe^{III}(TTP)Cl$ dissociates completely in solution. Therefore $[DMF]>10^5[Cl^-]$. Furthermore, in all probability, $k_{-1}>k_2$; thus, in the rate law, almost certainly $k_{-1}[DMF]\gg k_2[Cl^-]$. With this assumption, the rate law simplifies to Eq. (5). That is, for the outer-sphere mechanism proposed in Scheme 2, a first-order

$$\frac{d[Fe^{II}]}{dt} = k_{obs}[LMo^{IV}OCl(DMF)][Cl^-];$$

$$k_{obs} = \frac{k_1k_2}{k_{-1}[DMF]} \quad (5)$$

dependence on $[Cl^-]$ is predicted. To test this prediction, the rate of $Fe^{II}(TTP)$ formation was measured in the presence of a 10-fold excess (with respect to Fe^{III}) of added Cl^- (as tetrabutylammonium chloride). This addition had *no* effect on the reaction rate. If the reaction were first-order in Cl^- then the rate would have been expected to increase by at least a factor of 10. An even greater increase should have been observed if $Fe^{III}(TTP)Cl$ dissociation were not complete under the conditions studied.

Thus, the inner-sphere reaction pathway (Scheme 1) that couples chlorine atom transfer from $Fe^{III}Cl(TTP)$ to $LMo^{IV}OCl(DMF)$ to formal electron transfer from Mo(IV) to Fe(III) is most consistent with the available thermodynamic and kinetic data.

5. Conclusions

This work has demonstrated the coupling of an $Mo^{VI}O_2 \rightarrow Mo^{IV}O$ oxygen atom transfer reaction to a one-electron reoxidation of the resulting Mo(IV) center by a Fe(III) porphyrin center. However, the reoxidation step proceeds by an inner-sphere (halogen transfer) process, rather than by outer-sphere electron transfer. An inner-sphere reoxidation process is unlikely for sulfite oxidase (Fig. 1, step A) because the molybdenum and heme centers are likely to be kept well separated from one another by the protein backbone.

Acknowledgements

We gratefully acknowledge partial support of this research by the National Institutes of Health (GM-37773). We thank Drs Partha Basu, Michael Carducci and F.A. Walker for several helpful discussions and D. Myers for technical assistance.

References

[1] J.H. Enemark and C.G. Young, *Adv. Inorg. Chem., 40* (1993) 1.
[2] K.V. Rajagopalan, in M.P. Coughlan (ed.), *Molybdenum and Molybdenum-Containing Enzymes*, Pergamon, New York, 1980, p. 243.
[3] R.H. Holm, *Chem. Rev., 87* (1987) 1401.
[4] Z. Xiao, C.G. Young, J.H. Enemark and A.G. Wedd, *J. Am. Chem. Soc., 114* (1992) 9194.
[5] S. Trofimenko, *J. Am. Chem. Soc., 85* (1967) 6288.
[6] W.E. Cleland, Jr., K.M. Barnhart, K. Yamanouchi, D. Collison, F.E. Mabbs, R.B. Ortega and J.H. Enemark, *Inorg. Chem., 26* (1987) 1017.
[7] S.A. Roberts, C.G. Young, C.A. Kipke, W.E. Cleland, Jr., K. Yamanouchi, M.D. Carducci and J.H. Enemark, *Inorg. Chem., 29* (1990) 3650.
[8] A.D. Adler, F.R. Longo, J.D. Finarelli, J. Goldmacher, J. Assour and L. Korsakoff, *J. Organomet. Chem., 32* (1957) 476.
[9] A.D. Adler, F.R. Longo, F. Kampasand and J. Kim, *J. Inorg. Nucl. Chem., 32* (1970) 2443.
[10] F.A. Walker, V.E. Balke and G.A. McDermott, *J. Am. Chem. Soc., 104* (1982) 1569.
[11] S.A. Roberts, C.G. Young, W.E. Cleland, Jr., R.B. Ortega and J.H. Enemark, *Inorg. Chem., 27* (1988) 3044.

[12] F. Farchione, G.R. Hanson, C.G. Rodrigues, T.D. Bailey, R.N. Bagchi, A.M. Bond, J.R. Pilbrow and A.G. Wedd, *J. Am. Chem. Soc., 108* (1986) 831.
[13] C.J. Hinshaw and J.T. Spence, *Inorg. Chim. Acta, 125* (1986) L17.
[14] D. Dowerah, J.T. Spence, S. Raghuvir, A.G. Wedd, G.L. Wilson, F. Farchione, J.H. Enermark, J. Kristofzski and M. Bruck, *J. Am. Chem. Soc., 109* (1987) 5655.
[15] D. Brault, M. Rougee and M. Momenteau, *J. Chim. Physiochim. Biol., 68* (1971) 1621.
[16] D. Brault and M. Rougee, *Nature (London), 241* (1973) 19.
[17] D. Brault and M. Rougee, *Biochemistry, 13* (1974) 4591.
[18] D. Brault and M. Rougee, *Biochemistry, 13* (1974) 4599.
[19] K.J. Laidler, *Chemical Kinetics,* McGraw-Hill, New York, 1965.
[20] D.E. Over, S.C. Critchlow and J.M. Mayer, *Inorg. Chem., 31* (1992) 4643.
[21] P.J. Desrochers, K.W. Nebesny, M.J. Labarre, M.A. Bruck, G.F. Neilson, R.P. Sperline, J.H. Enemark, G. Backes and K. Wieghardt, *Inorg. Chem., 33* (1994) 15.
[22] S. Ferguson-Miller and E. Margolesh, in D. Dolphin (ed.), *The Porphyrins,* Academic Press, New York, 1979, Ch. 7, p. 149.
[23] T.E. Meyer and M.D. Kamen, *Adv. Protein Chem., 35* (1982) 105.
[24] I.A. Cohen, *J. Am. Chem. Soc., 91* (1969) 1980.
[25] I.A. Cohen and J. Brown, *J. Am. Chem. Soc., 94* (1972) 4255.
[26] I.A. Cohen, *Ann. N.Y. Acad. Sci., 203* (1970) 453.
[27] I.A. Cohen, C. Jung and T. Governo, *J. Am. Chem. Soc., 94* (1972) 3003.
[28] L.K. Woo, J.A. Hays and J.G. Goll, *Inorg. Chem., 29* (1990) 3916.
[29] D.A. Summerville and I.A. Cohen, *J. Am. Chem. Soc., 98* (1976) 1747.
[30] L.K. Woo and J.G. Goll, *J. Am. Chem. Soc., 111* (1989) 3755.
[31] D.W. Dixon, M. Barbush and A. Shirozi, *Inorg. Chem., 24* (1985) 1081.
[32] R.D. Chapman and E.B. Fleischer, *J. Am. Chem. Soc., 104* (1982) 1582.
[33] L.A. Bottomley and K.M. Kadish, *Inorg. Chem., 20* (1981) 1348.
[34] K.M. Kadish and R.K. Rhodes, *Inorg. Chem., 22* (1983) 1090.
[35] K.M. Kadish and L.A. Bottomley, *Inorg. Chem., 19* (1980) 832.
[36] K.M. Kadish and L.A. Bottomley, *Anal. Chim. Acta, 139* (1982) 367.
[37] R. Quinn, M. Nappa and J.S. Valentine, *J. Am. Chem. Soc., 104* (1982) 2588.
[38] D. Lexa, M. Momenteau, P. Rentien, G. Rytz, J.M. Saveant and G. Lang, *J. Am. Chem. Soc., 106* (1984) 4755.
[39] C.A. Reed, T. Mashiko. S.P. Bentley, M.E. Kastner, W.R. Scheidt, K. Spartalian and G. Lang, *J. Am. Chem. Soc., 101* (1979) 2948.
[40] S.B. Brown and I.R. Lantzke, *Biochem. J., 115* (1969) 279.
[41] F.A. Walker, M.W. Lo and M.T. Ree, *J. Am. Chem. Soc., 98* (1976) 5552.